

Crack analysis by using an extended meshfree method and cartesian transformation method without creating subdomains

Vay Siu Lo^{1,2}, Hien Thai Nguyen^{1,2}, Thien Tich Truong^{1,2}, Nha Thanh Nguyen^{1,2,*}

ABSTRACT

This paper investigates the fracture behavior of 2-dimensional plates with through-thickness crack by using the extended concept of the Radial Point Interpolation Method (RPIM). The attractiveness of the RPIM shape functions is the satisfaction of the Kronecker delta property providing direct imposition of essential boundary conditions. In the extended concept, the jump in deflection and rotation fields caused by crack, also the stress singularity near the crack tip are described by adding enriched functions to the interpolation equation. Particularly, Heaviside function and asymptotic enriched function. For numerical integration, the Cartesian Transformation Method (CTM) is employed. No integration background cell is required in CTM, this technique transforms a domain integral into a boundary integral and a 1D integral. For analysis of discontinuous problems, in this study, the distribution of integration points is manipulated to avoid the discontinuity caused by crack segmentation. Therefore, no subdomains are required, unlike other reference CTM studies. To achieve that, a virtual boundary is introduced that represents the discontinuity such as holes or cracks. This also matches the concept of the extended approach that no explicit discontinuity exists in the geometry, instead, the discontinuity is modelled by mathematics equation. The Stress Intensity Factors (SIFs) of the crack problems are evaluated through the interaction integral technique. The efficiency of the proposed method is illustrated through various numerical examples. The accuracy of the obtained results are compared with other available numerical solutions and analytical solutions.

Key words: Crack analysis, extended meshfree method, XRPIM, CTM

¹Department of Engineering Mechanics, Faculty of Applied Sciences, Ho Chi Minh City University of Technology (HCMUT), 268 Ly Thuong Kiet Street, District 10, Ho Chi Minh City, Vietnam

²Vietnam National University Ho Chi Minh City, Linh Trung Ward, Thu Duc City, Ho Chi Minh City, Vietnam

Correspondence

Nha Thanh Nguyen, Department of Engineering Mechanics, Faculty of Applied Sciences, Ho Chi Minh City University of Technology (HCMUT), 268 Ly Thuong Kiet Street, District 10, Ho Chi Minh City, Vietnam

Vietnam National University Ho Chi Minh City, Linh Trung Ward, Thu Duc City, Ho Chi Minh City, Vietnam

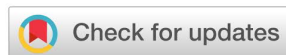
Email: nhanguyen@hcmut.edu.vn

History

- Received: 16-12-2022
- Accepted: 09-9-2023
- Published Online: 31-12-2023

DOI :

<https://doi.org/10.32508/stdjet.v6iSI2.1067>



INTRODUCTION

The finite element method (FEM) has been popularly used in various engineering fields such as structural analysis, topology optimization, heat transfer. Besides, fracture analysis is also one of the most interested topics since it is related to the durability and lifetime of the structure. However, using FEM to model crack is quite complicated due to the discontinuity of the geometry and the singularity of the stress field asymptotic to the crack tip. Furthermore, as the crack grows, the mesh needs to be updated at each calculation step. This remeshing task is time-consuming. For that reason, the extended finite element method (XFEM)¹ is proposed to model discontinuity such as crack, hole, etc by a mathematical approach and crack propagation can be simulated without remeshing. The enrichment functions are used in the XFEM formulation to capture the displacement field discontinuity across the crack and the stress field singularity near the crack tip.

In addition to the development of mesh-based methods like FEM, the meshfree method is another class of numerical method that being noticed and thriving recently. As the name implies, no element is

found in meshfree method, the problem domain is discretized into a set of scattering nodes. Since the last two decades, many meshfree methods have been introduced such as the Element Free Galerkin (EFG)^{2,3}, Smoothed Particle Hydrodynamics (SPH)⁴, Moving Kriging (MK)^{5,6}, Radial Point Interpolation Method (RPIM)⁷⁻¹⁰, etc. Unlike many other meshfree methods, RPIM possesses the Kronecker delta property. For that reason, it is easy to impose the essential boundary conditions as in the traditional FEM which is not capable for other meshfree methods. And to investigate the fracture behavior, Nguyen et al. developed the extended RPIM (XRPIM)^{9,11-13} based on the idea of XFEM. Other meshfree methods without using the “extended” concept for analyzing fracture problems can be mentioned as the Integrated Local Mesh Free model (ILMF)¹⁴ and Weighted Least Squares method (WLS)¹⁵.

In the meshfree method, the numerical integration is mainly computed using the Gaussian quadrature (GQ) and conducted on a background grid. This technique may lead to numerical error as pointed out by^{9,10}. To overcome this, Khosravifard et al.^{16,17} proposed the Cartesian transformation method (CTM)

Cite this article : Lo V S, Nguyen H T, Truong T T, Nguyen N T. Crack analysis by using an extended meshfree method and cartesian transformation method without creating subdomains. *Sci. Tech. Dev. J. – Engineering and Technology* 2023; 5(SI2):33-43.

Copyright

© VNUHCM Press. This is an open-access article distributed under the terms of the Creative Commons Attribution 4.0 International license.



as an alternative numerical integration technique. The CTM technique can be applied even in domains with complicated shape and does not require creating background cells. Besides the original potential of the technique, the CTM was also incorporated NURBS^{18,19} to deal with complex configurations. Then, CTM is also implemented to analyze 2D cracked problems in¹³. However, to ensure the accuracy of the technique, the integral domain must not be discontinuous due to the appearance of the crack. Therefore, in previous studies^{9,13}, it requires creating subdomain to make sure that the integration ray is not separated by the crack. More specifically, the crack is at the boundary of the subdomain. This approach is suitable and convenient for simulating static crack, but there would be difficulties when the crack propagates.

In this study, the authors follow the original idea of CTM to create integration points. The integration interval in each integration ray is manipulated to avoid the crack, this ensures the continuity of the integral domain. Hence, there is no need to create subdomains. Besides, the region close to the crack needs many integration points to obtain good approximations, so the distribution of integration points in this zone is also modified to get more points near the crack. It should also be noted that, in the extended concept, there is no explicit crack in the model, so the crack boundary used when manipulating the CTM integral point generation process is a “virtual discontinuous boundary”.

This paper introduces the manipulation of CTM to compute numerical integration without creating subdomains for analysis of cracked bodies. The XRPIM is employed for modelling cracks. The fracture parameters needed to be evaluated are the stress intensity factors (SIFs), which are calculated using the interaction integral approach. The accuracy of the technique is shown by various numerical examples, proving the validity of the method.

METHODOLOGY

Extended Radial Point Interpolation Method

In the XRPIM formulation, the approximate displacement field $u^h(x)$ at an interest point x is expressed as the equation below¹¹⁻¹³

$$u^h(x) = \sum_{i \in W} \phi_i(x) u_i + \sum_{j \in W_s} \phi_j(x) (H - H_j) b_j + \sum_{k \in W_t} \phi_k(x) [\sum_{l=1}^4 (F_l - F_{lk}) c_{lk}]$$

in which the step by step to construct the RPIM shape function ϕ_i can be found in²⁰. W denotes the set of all

nodes inside the support domain of the interest point x , W_s collects split nodes that have support domains cut by the crack and W_t contains tip nodes that contains crack tip in the support domain (see Figure 1). For the enrichment part, the value of Heaviside function H is defined as the following equation

$$H(f(x)) = \begin{cases} +1 & \text{if } f(x) > 0 \\ -1 & \text{if } f(x) < 0 \end{cases} \quad (2)$$

The tip-enriched function F_I is defined as¹

$$F_I(r, \theta) = \{ \sqrt{r} \sin \frac{\theta}{2}, \sqrt{r} \cos \frac{\theta}{2}, \sqrt{r} \sin \frac{\theta}{2} \sin \theta, \sqrt{r} \cos \frac{\theta}{2} \sin \theta \} \quad (3)$$

where r and θ are illustrated in Figure 1.

To compute the stiffness matrix of the cracked body, the strain computing matrix B is now including the standard $B^{standard}$ and enriched $B^{enriched}$ constituents

$$B = [B^{standard}, B^{enriched}] \quad (4)$$

The enriched matrix $B^{enriched}$ for split nodes and tip nodes are given as

$$B^{split\ enr} = \begin{bmatrix} [\phi_I(H - H_I)]_{,1} & 0 \\ 0 & [\phi_I(H - H_I)]_{,2} \end{bmatrix} \quad (5)$$

$$B^{tip\ enr, l} = \begin{bmatrix} [\phi_I(F_I - F_{Il})]_{,1} & 0 \\ 0 & [\phi_I(F_I - F_{Il})]_{,2} \\ [\phi_I(F_I - F_{Il})]_{,2} & [\phi_I(F_I - F_{Il})]_{,1} \end{bmatrix} \quad (6)$$

In fracture analysis, stress intensity factors (SIFs) play an important role and need to be evaluated. The SIFs values are usually computed by the interaction integral approach¹ which is defined as the following expression

$$I = \int_A (\delta_{ij} u_{i,1}^{aux} + \delta_{ij}^{aux} u_{i,1} - W^{int} \delta_{1j}) q_{,j} dA \quad (7)$$

where the auxiliary state is expressed by the superscript “aux”. The auxiliary fields can be found in¹. q is a weight function and defined as the following expression

$$q = \left(1 - 2 \frac{|x_1 - x_1^{tip}|}{c} \right) \left(1 - 2 \frac{|x_2 - x_2^{tip}|}{c} \right) \quad (8)$$

in which c denotes the side length of the square domain having the crack-tip as its center.

The interaction strain energy is computed as below

$$W^{int} = \frac{1}{2} (\delta_{ij} \epsilon_{ij}^{aux} + \delta_{ij}^{aux} \epsilon_{ij}) \quad (9)$$

The SIFs can be derived by using the relation

$$I = \frac{2(K_I K_I^{aux} + K_{II} K_{II}^{aux})}{\bar{E}} \quad (10)$$

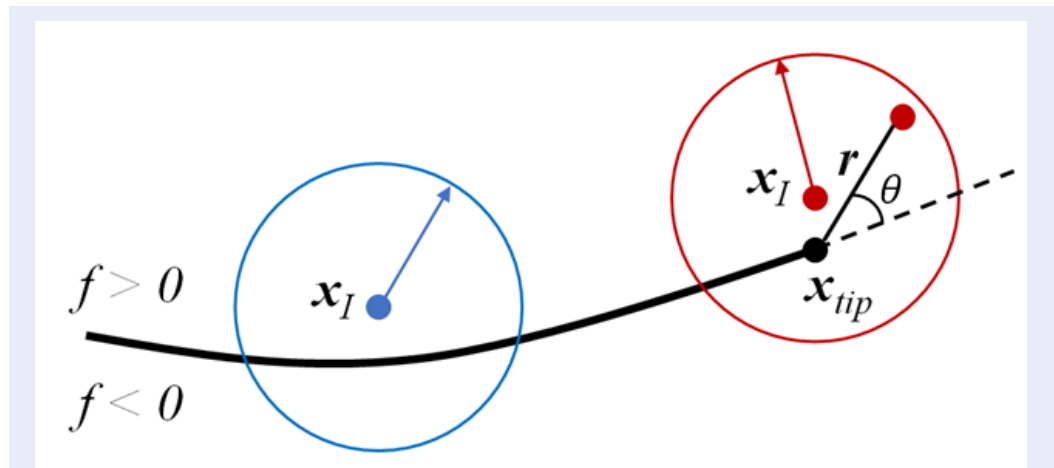


Figure 1: Types of enriched nodes and local polar coordinate at the crack tip. Blue dot indicates split node and red dot is the tip node.

for example, the opening mode SIF K_I is obtained by setting $K_I^{aux} = 1$ and $K_{II}^{aux} = 1$. The term \bar{E} in Eq. (10) is defined as

$$\begin{cases} \bar{E} = E \text{ plane stress} \\ \bar{E} = E / (1 - \nu^2) \text{ plane strain} \end{cases} \quad (11)$$

Cartesian Transformation Method

To simplify the ideas for the proposed method, a 2D integration domain Ω that contains a hole inside is considered. The domain integral M of a function $F(x, y)$ over the domain Ω can be described as the equation below

$$M = \int_{\Omega} F(x, y) d\Omega \quad (12)$$

Now create an auxiliary domain Ω_A containing the initial domain, see Figure 2. One can use any arbitrary shapes for the domain Ω_A ^{16,17}, but a rectangular domain should be chosen for the simplicity. Define a function $\bar{F}(x, y)$ in the whole domain Ω_A as below

$$\bar{F}(x, y) = \begin{cases} F(x, y) & (x, y) \in \Omega \\ 0 & (x, y) \notin \Omega \end{cases} \quad (13)$$

Due to the rectangular domain, the integral in Eq. (12) is rewritten as^{16,17}

$$M = \int_{y_1}^{y_2} \int_a^b \bar{F}(x, y) dx dy = \int_{y_1}^{y_2} h(y) dy \quad (14)$$

The Gaussian quadrature (GQ) is employed to compute the 1D integral in Eq. (14)

$$\begin{aligned} M &= \sum_{i=1}^n \left(\int_{y_i}^{y_{i+1}} h(y) dy \right) = \sum_{i=1}^n \left(\int_{-1}^1 h(\eta) J d\eta \right) \\ &= \sum_{i=1}^n \sum_{j=1}^m h(\eta_j) J w_j \end{aligned}$$

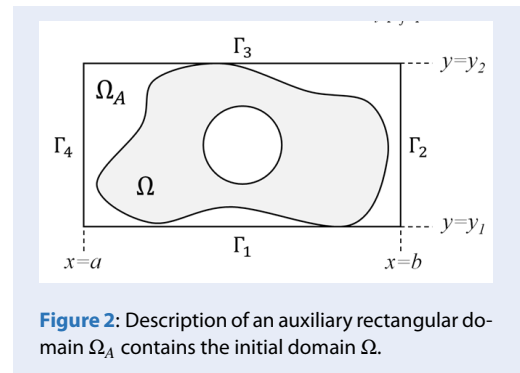


Figure 2: Description of an auxiliary rectangular domain Ω_A contains the initial domain Ω .

In Eq. (15), $h(y) = h(y(\eta))$, η_j stands for the j th integration point (see Figure 3 (a)), w_j denotes the weight number of the j th integration point and $J = dy/d\eta = (y_{i+1} - y_i)/2$.

Draw an integration ray through the j th Gaussian point η_j , parallel with the horizontal axis and cross the domain Ω ¹⁶. Now the integral $h(y) = \int_a^b \bar{F}(x, y) dx$ in each integration ray is computed by using the GQ

$$\begin{aligned} h(y_i) &= \int_a^b \bar{F}(x, y_i) dx \\ &= \sum_{q=1}^k \left(\int_{x_{2q-1}}^{x_{2q}} F(x, y_i) dx \right) \end{aligned} \quad (16)$$

$$\begin{aligned} \int_{x_{2q-1}}^{x_{2q}} F(x, y_i) dx &= \sum_{s=1}^l \left(\int_{-1}^1 F(\xi, y_i) J d\xi \right) \\ &= \sum_{q=1}^k \sum_{s=1}^l F(\xi_s, y_i) J w_s \end{aligned} \quad (17)$$

where (ξ_s, y_i) is the s th integration point on the i th integration ray, w_s is the weight number of the point (ξ_s, y_i) and $J = (x_{2q} - x_{2q-1})/2$.

In previous reference studies^{9,13}, to ensure the continuity of the integration domain, particularly the inte-

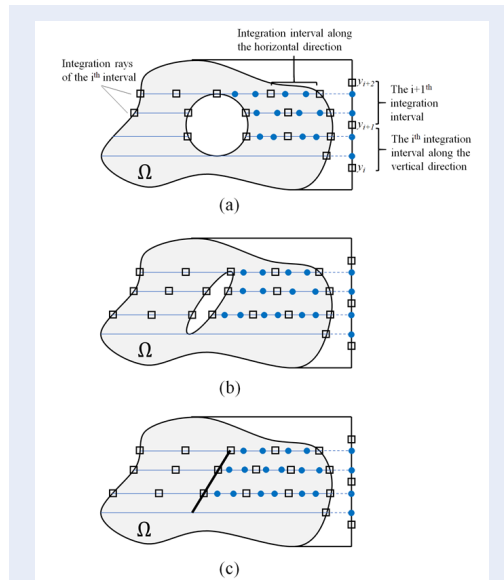


Figure 3: Description of integration intervals, rays and points.

gration interval, the whole body is divided into subdomains. The crack is at the boundary of the subdomain as shown in Figure 4. This approach is suitable and convenient for simulating static crack, but there would be difficulties when the crack propagates. For that reason, this paper aims to introduce a so-called “manipulated CTM” for computing the numerical integration without creating subdomains.

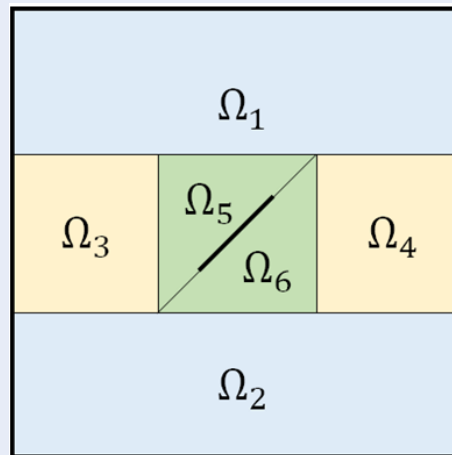


Figure 4: An example of subdomains for CTM integration in a cracked plate.

Now considering the circular hole in the integration domain Ω (Figure 3(a)) becomes slender as in Fig-

ure 3(b) and then becomes a straight line as in Figure 3(c). The boundary of the interval on two sides of the circle (square marker) is now combined into one. The integration intervals on two sides of the straight line (or crack) are now continuous. However, in the “extended” concept of the meshfree method, no explicit crack in the geometry is performed. Therefore, the discontinuity is now considered as a “virtual boundary” (see Figures 3 and 5). This virtual discontinuous boundary is for defining enriched nodes and the integration intervals. Overall, the geometry of the problem remains intact.

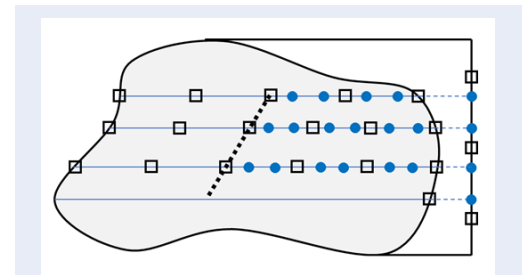


Figure 5: “Virtual boundary” of crack.

For illustration, Figure 6 shows the distribution of integration points in a square domain with an inclined crack. As seen in the figure, the region around the crack is manipulated to have a large number of integral points. More details on the procedure of distributing these integration points are discussed in Section discussions.

Notice that for a horizontal crack that parallels the integration ray, it is easy to manipulate the integration ray not coincident with the crack and then no treatment is needed. Figure 7 shows two approaches of creating integration points when the crack parallels the integration ray. If the integration ray does not coincide with the crack as in Figure 7(a), this can be considered as an ordinary CTM. When the integration ray coincides with the crack, the boundary of the interval must be defined as the crack tip as in Figure 7(b).

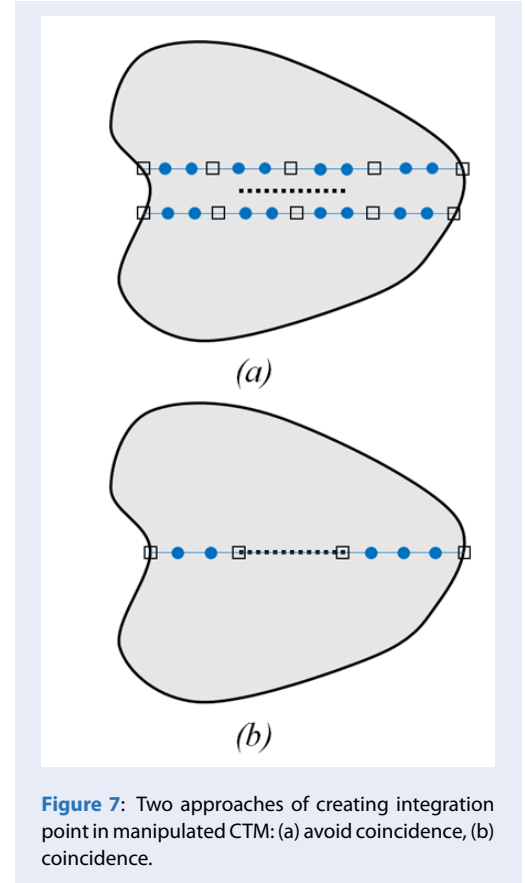
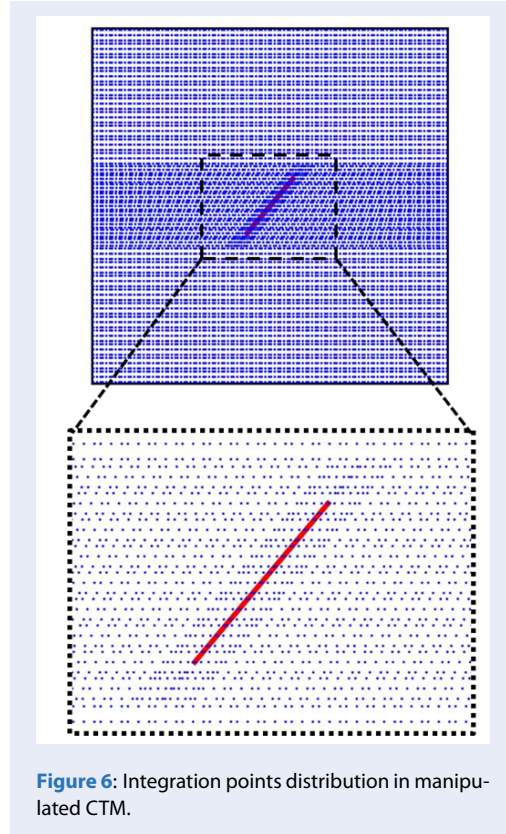
The implementation procedure is summarized in Table 1. Compared with the original CTM, only steps 3 and 4 are inserted, steps 2 and 6 are also slightly modified.

RESULTS

As mentioned above, for the horizontal crack that parallels to the x -axis (and integration rays), it is convenient to create integration points avoiding the crack. Therefore, two numerical examples of inclined crack

Table 1: Summary of the implementation procedure

<p>Step 1. Create integration intervals on the y-axis and define the position of integration rays.</p> <p>Step 2. Create integration rays, more rays in the region of crack.</p> <p>Step 3. Check if the current integration ray intersects with crack. If “Yes”, move to Step 4, if “No”, move to Step 5.</p> <p>Step 4. Define the intersect locations.</p> <p>Step 5. Create integration intervals on each ray.</p> <p>Step 6. Creating integration points, more points in the interval adjacent to the crack.</p>



model are investigated in this part to present the efficiency of the proposed method, particularly:

- Square plate with slant crack at center.
- Rectangular plate with a slant edge crack.

Square plate with slant crack at center

In this first example, a square plate of side $2b = 2$ m with a slant crack (see Figure 8) is examined. The crack length is $2a = 0.2$ m. The plate is subjected to distributed force $\delta_0 = 1$ Pa on top and bottom edges. The material properties are $E=1000$ Pa and $\nu = 0.3$, and the plane strain state is assumed. The discretized model of 50×50 nodes is consider for this problem.

The distribution of integration points is similar to the illustration in Figure 6.

The accuracy of the XRPIM approach with the manipulated CTM is shown by the comparison between the obtained stress intensity factors K_I and K_{II} with the analytical solutions. According to¹, the analytical solution for SIFs is found as

$$\begin{aligned} K_I &= \delta_0 \sqrt{\pi a} \cos^2 \beta, \\ K_{II} &= \delta_0 \sqrt{\pi a} \cos \beta \sin \beta. \end{aligned} \tag{18}$$

where β is the crack angle as shown in Figure 8. The change of the stress intensity factors K_I and K_{II} versus angle of inclination β is displayed in Figure 9.

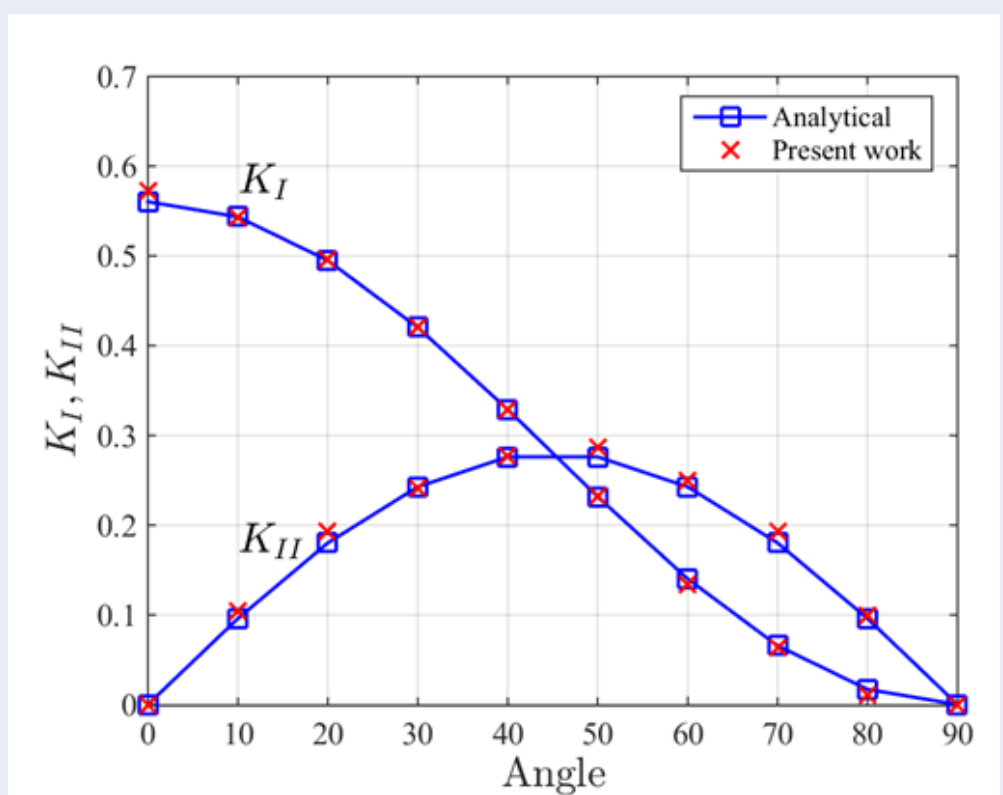


Figure 9: Variation of the SIFs K_I, K_{II} versus the crack angle β .

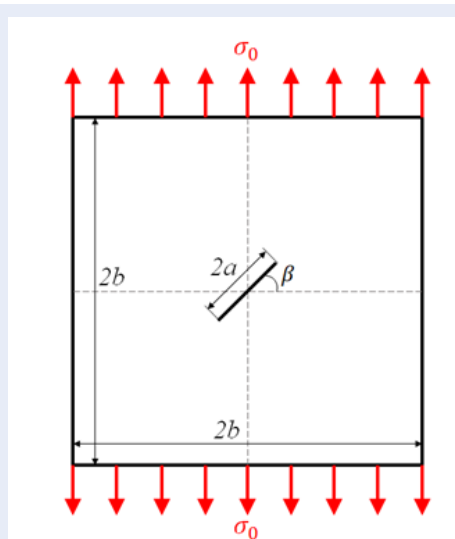


Figure 8: Square plate with slant crack at center.

The obtained results given by the present approach fit well with reference ones. It can be concluded that the manipulated CTM has high accuracy. However,

a slight deviation is observed in the figure, which can be explained that the number of integration points in the region around the crack is not sufficiently large. This can be solved by increasing the number of integration rays and points in the intervals near the crack. Of course, the computational cost will also increase. The figure also shows that when the orientation angle β increases, K_I decreases. Meanwhile K_{II} increases and decreases symmetrically. The distribution of von Mises stress is shown in Figure 10 for the case of inclined angle $\beta = 60^\circ$. It is easy to observe the stress concentration at the two crack tips.

Rectangular plate with a slant edge crack

In this example, a rectangular plate of dimension $b \times 2b = 1 \times 2m$ containing an inclined crack at the left edge (see Figure 11) is considered. The plate is subject to distributed force $\delta_0 = 1 Pa$ on top and bottom edges. The plane strain state is assumed and material properties are elastic modulus $E = 1000 Pa$ and Poisson's ratio $\nu = 0.3m$, and. The model is discretized uniformly with 30×60 nodes. The inclined angle is $\beta = 30^\circ$, various crack lengths are examined. The obtained results are compared to XFEM results. The XFEM model used 29×59 Q4 elements (also

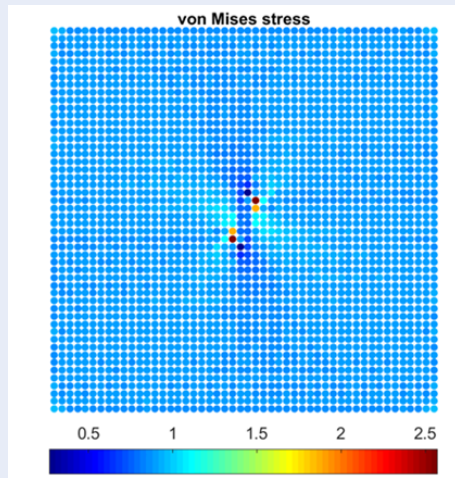


Figure 10: von Mises stress distribution for $\beta = 60^\circ$. Unit: Pa.

has 30×60 nodes). Figure 11 illustrates the discrete model of XFEM and XRPIM in the case of $a/b = 0.6$.

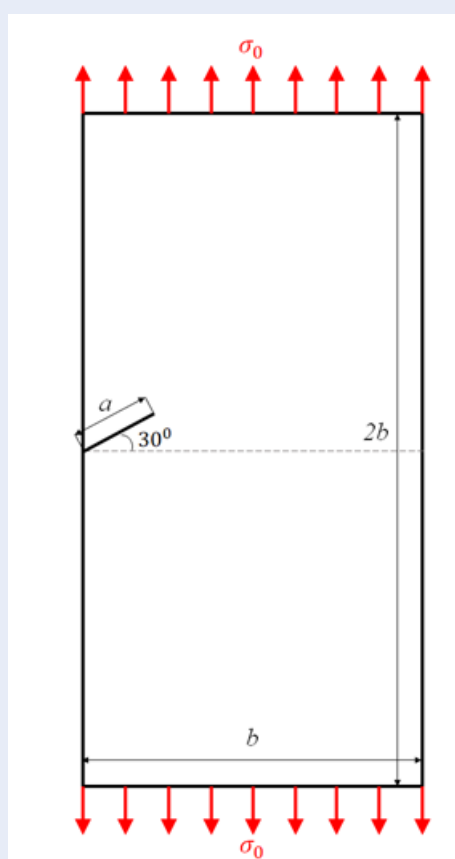


Figure 11: Model of a rectangular plate with a slant edge crack under tension.

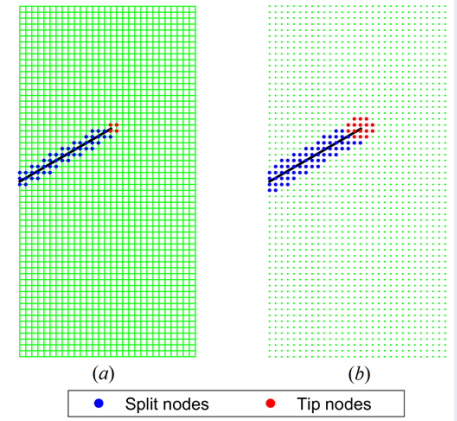


Figure 12: Discrete model when $a/b = 0.6$. (a) XFEM and (b) XRPIM.

The plots in Figure 13 show the variation of the normalized stress intensity factors K_I and K_{II} versus the a/b ratio. It can be observed that results given by the current approach fit well with reference results from XFEM. The figure also shows that K_I and K_{II} increases when the length of crack increases. For $\beta = 30^\circ$, the opening mode K_I is dominant, this is also consistent with the observations in the previous example.

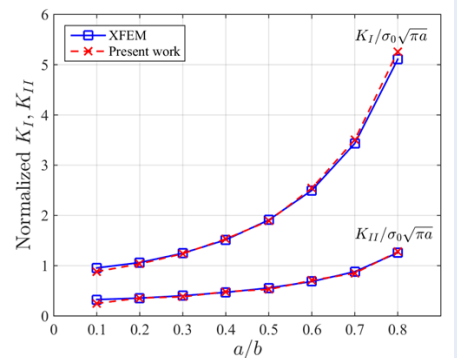


Figure 13: Variation of normalized K_I and K_{II} with respect to the a/b ratio.

Figure 14 illustrates the distribution of total displacement field in three different a/b ratios. It can be seen that when the crack length is small compared to the width of the plate (Figure 14 (a)), the total displacement field seem symmetry on two sides of the plate. And when the crack length increases, the total displacement dominant distributed on the top of the plate and above the crack.

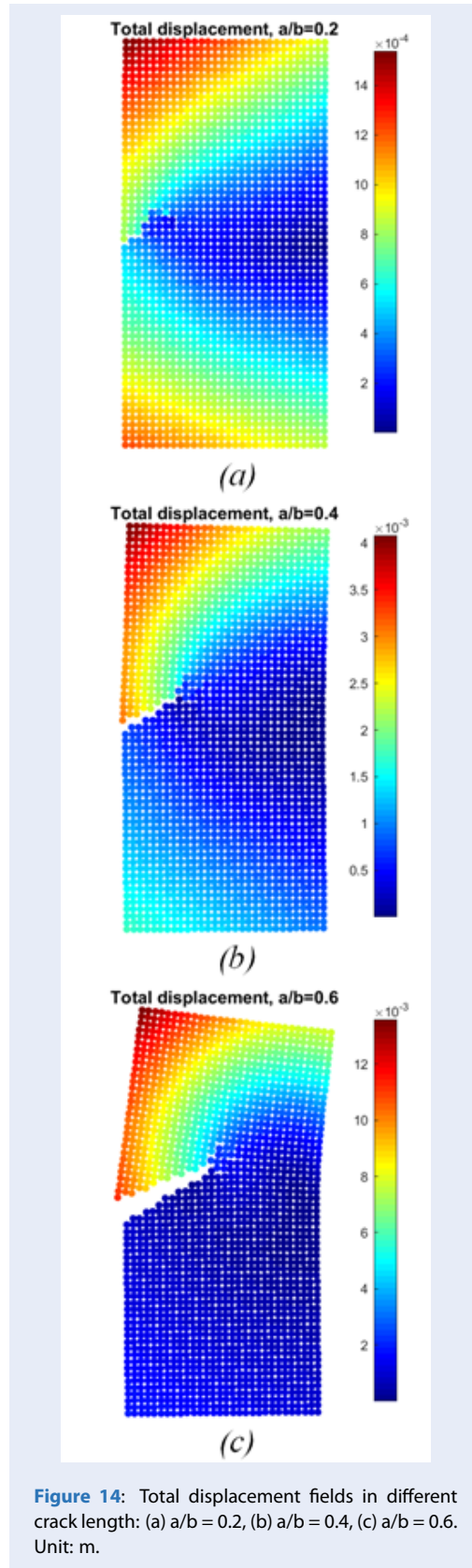


Figure 14: Total displacement fields in different crack length: (a) $a/b = 0.2$, (b) $a/b = 0.4$, (c) $a/b = 0.6$. Unit: m.

Figure 15 displays the von Mises stress field in three different a/b ratios. Based on the figure, the singularity of stress is clearly recognized at the crack-tip.

DISCUSSIONS

The integration points as shown in Figure 6 is created according to the steps in Table 1. Firstly, when creating integration intervals in the y-direction, determine which intervals have at least one boundary point in the region of the crack. Particularly in Fig. 6, the crack zone is determined by the vertical distance between two crack tips and extending by $2a/3$ (a is half crack length). Intervals that are in the crack zone have more integration rays. Then, when determining the intersection of the integration rays and the crack, those intervals in the x-direction with a boundary point at the intersection have more integration points distributed in that interval. Finally, we get the result as shown in Figure 6 without having to split the domain into sub-domains.

As presented in section results, the results obtained from the present approach show a good agreement with those from analytical solutions and XFEM. The trending variation of SIFs versus the angle orientation and crack length is also observed from the numerical results.

For the case of central crack, the following conclusion can be drawn: when the orientation angle β increases, K_I decreases. Meanwhile K_{II} increases and decreases symmetrically.

For the case of edge crack, the result shows that K_I and K_{II} increases when the length of crack increases. For β , the opening mode is dominant, this is also consistent with the observations in the central crack case. When the crack length is small compared to the width of the plate, the total displacement field seem symmetry on two sides of the plate. And when the crack length increases, the total displacement dominant distributed on the top of the plate and above the crack.

The results obtained by the present approach are in good agreement with reference ones. It can be concluded that the manipulated CTM has high accuracy. However, a slight deviation is observed in both examples, which can be explained that the number of integration points in the region around the crack is not sufficiently large. This can be solved by increasing the number of integration rays and the number of integration points in the intervals near the crack. Of course, the computational cost will also increase.

The procedure of this “manipulated CTM” is similar to the original one. Hence, with the existing CTM code, only slight modifications are required.

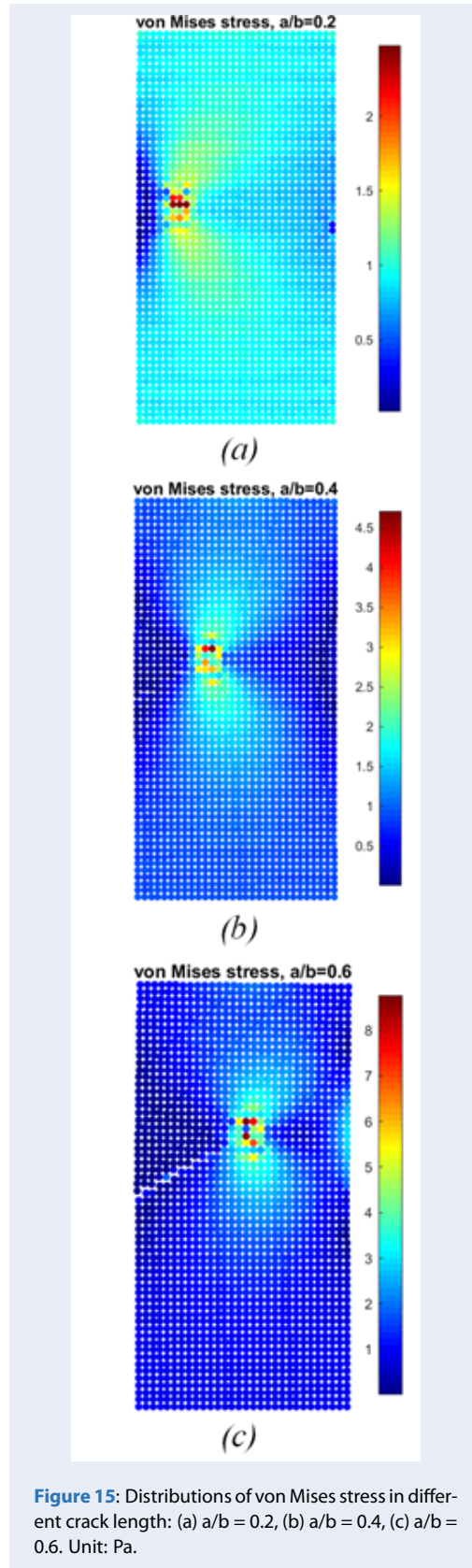


Figure 15: Distributions of von Mises stress in different crack length: (a) $a/b = 0.2$, (b) $a/b = 0.4$, (c) $a/b = 0.6$. Unit: Pa.

CONCLUSIONS

The extended RPIM has been employed to investigate 2D cracked problems in this study. The RPIM possesses the Kronecker delta property of shape functions, allowing the direct imposition of the essential boundary conditions as in the conventional FEM. For numerical integration, the CTM is applied in which there is no integration background cell is required. This technique transforms a 2D domain integral into a boundary integral and a 1D integral. For crack analysis in this study, the distribution of integration points is controlled to avoid the discontinuity at crack. As a result, there is no subdomain are needed, unlike other previous CTM applications. With the existing CTM code, only slight modifications are required since the current technique is similar to the original one.

The accuracy of the present method is demonstrated through the evaluation of the stress intensity factors. The proposed approach has the potential to solve more complicated problems, such as crack propagation, dynamic fracture and nonlinear problems (material and geometry). To do so, the current algorithm needs to be further modified and developed in the next studies.

ACKNOWLEDGMENT

This research is funded by Vietnam National University Ho Chi Minh City (VNU-HCM) under grant number B2022-20-02. We acknowledge Ho Chi Minh City University of Technology (HCMUT), VNU-HCM for supporting this study.

ABBREVIATIONS

- CTM: Cartesian Transformation Method
- EFG: Element Free Galerkin.
- FEM: Finite Element Method.
- MK: Moving Kriging.
- RPIM: Radial Point Interpolation Method.
- SIF: Stress intensity factor.
- SPH: Smoothed Particle Hydrodynamics.
- XFEM: eXtended Finite Element Method.
- XRPM: eXtended Radial Point Interpolation Method.

CONFLICT OF INTEREST

Group of authors declare that this manuscript is original, has not been published before and there is no conflict of interest in publishing the paper.

AUTHOR CONTRIBUTION

Vay Siu Lo is the developer of the numerical method and does as the manuscript editor.

Hien Thai Nguyen takes part in gathering datas and verifying the numerical solution.

Thien Tich Truong works as the supervisor and contributes ideas for the numerical method.

Nha Thanh Nguyen provides the main ideas for the proposed method, checking the manuscript and also funding acquisition.

REFERENCES

1. Moes N, Dolbow J, Belytschko T. A finite element method for crack growth without remeshing. *Int J Numer Methods Eng.* 1999;46(1):131-50; Available from: [https://doi.org/10.1002/\(SICI\)1097-0207\(19990910\)46:1<131::AID-NME726>3.0.CO;2-J](https://doi.org/10.1002/(SICI)1097-0207(19990910)46:1<131::AID-NME726>3.0.CO;2-J).
2. Belinha J, Dinis LMJS. Analysis of plates and laminates using the elementfree Galerkin method. *Comput Struct.* 2006;84(22-23):1549-59; Available from: <https://doi.org/10.1016/j.compstruc.2006.01.013>.
3. Peng LX, Liew KM, Kitipornchai S. Analysis of stiffened corrugated plates based on the FSDT via the mesh-free method. *Int J Mech Sci.* 2007;49(3):364-78; Available from: <https://doi.org/10.1016/j.ijmecsci.2006.08.018>.
4. Monaghan JJ. Smoothed particle hydrodynamics. *Annu Rev Astron Astrophys.* 1992;30(1):543-74; Available from: <https://doi.org/10.1146/annurev.aa.30.090192.002551>.
5. Bui TQ, Nguyen MN, Zhang C. Buckling analysis of Reissner-Mindlin plates subjected to in-plane edge loads using a shear-locking-free and meshfree method. *Eng Anal Bound Elem.* 2011;35(9):1038-53; Available from: <https://doi.org/10.1016/j.enganabound.2011.04.001>.
6. Bui TQ, Doan DH, Van Do T, Hirose S, Duc ND. High frequency modes meshfree analysis of Reissner-Mindlin plates. *J Sci Adv Mater Dev.* 2016;1(3):400-12; Available from: <https://doi.org/10.1016/j.jsamd.2016.08.005>.
7. Wang JG, Liu GR. A point interpolation meshless method based on radial basis functions. *Int J Numer Methods Eng.* 2002;54(11):1623-48; Available from: <https://doi.org/10.1002/nme.489>.
8. Liew KM, Chen XL. Mesh-free radial point interpolation method for the buckling analysis of Mindlin plates subjected to in-plane point loads. *Int J Numer Methods Eng.* 2004;60(11):1861-77; Available from: <https://doi.org/10.1002/nme.1027>.
9. Truong TT, Lo VS, Nguyen MN, Nguyen NT, Nguyen DK. Evaluation of fracture parameters in cracked plates using an extended meshfree method. *Eng Fract Mech.* 2021;247:107671; Available from: <https://doi.org/10.1016/j.engfracmech.2021.107671>.
10. Truong TT, Lo VS, Nguyen MN, Nguyen NT, Nguyen KD. A novel meshfree Radial Point Interpolation Method with discrete shear gap for nonlinear static analysis of functionally graded plates. *Eng Comput.* 2023;39(4):2989-3009; Available from: <https://doi.org/10.1007/s00366-022-01691-w>.
11. Nguyen NT, Bui TQ, Zhang C, Truong TT. Crack growth modeling in elastic solids by the extended meshfree Galerkin radial point interpolation method. *Eng Anal Bound Elem.* 2014;44:87-97; Available from: <https://doi.org/10.1016/j.enganabound.2014.04.021>.
12. Nguyen NT, Bui TQ, Truong TT. Transient dynamic fracture analysis by an extended meshfree method with different crack-tip enrichments. *Meccanica.* 2017;52(10):2363-90; Available from: <https://doi.org/10.1007/s11012-016-0589-6>.
13. Nguyen NT, Bui TQ, Nguyen MN, Truong TT. Meshfree thermomechanical crack growth simulations with new numerical integration scheme. *Eng Fract Mech.* 2020;235:107121; Available from: <https://doi.org/10.1016/j.engfracmech.2020.107121>.
14. Oliveira T, Véliz W, Santana E, Araújo T, Mendonça F, Portela A. A local mesh free method for linear elasticity and fracture mechanics. *Eng Anal Bound Elem.* 2019;101:221-42; Available from: <https://doi.org/10.1016/j.enganabound.2019.01.007>.
15. Elmhaia O, Belaasilia Y, Askour O, Braikat B, Damil N. An efficient mesh-free approach for the determination of stresses intensity factors. *Eng Anal Bound Elem.* 2021;133:49-60; Available from: <https://doi.org/10.1016/j.enganabound.2021.08.001>.
16. Khosravifard A, Hematiyan MR. A new method for meshless integration in 2d and 3d galerkin meshfree methods. *Eng Anal Bound Elem.* 2010;34(1):30-40; Available from: <https://doi.org/10.1016/j.enganabound.2009.07.008>.
17. Khosravifard A, Hematiyan MR, Marin L. Nonlinear transient heat conduction analysis of functionally graded materials in the presence of heat sources using an improved meshless radial point interpolation method. *Appl Math Modell.* 2011;35(9):4157-74; Available from: <https://doi.org/10.1016/j.apm.2011.02.039>.
18. Nguyen MN, Nguyen NT, Truong TT, Bui TQ. An efficient reduced basis approach using enhanced meshfree and combined approximation for large deformation. *Eng Anal Bound Elem.* 2021;133:319-29; Available from: <https://doi.org/10.1016/j.enganabound.2021.09.007>.
19. Nguyen NT, Nguyen MN, Vu TV, Truong TT, Bui TQ. A meshfree model enhanced by NURBS-based Cartesian transformation method for cracks at finite deformation in hyperelastic solids. *Eng Fract Mech.* 2022;261:108176; Available from: <https://doi.org/10.1016/j.engfracmech.2021.108176>.
20. Liu GR. Meshfree methods: moving beyond the finite element method. Boca Raton: CRC Press; 2010;.

Phân tích nứt bằng một phương pháp không lưới mở rộng và phương pháp biến đổi Đê-các không cần tạo miền con

Lồ Sùi Vỹ^{1,2}, Nguyễn Thái Hiền^{1,2}, Trương Tích Thiện^{1,2}, Nguyễn Thanh Nhã^{1,2,*}

TÓM TẮT

Bài báo này nghiên cứu ứng xử rạn nứt của các tấm phẳng có vết nứt xuyên suốt chiều dày bằng cách sử dụng dạng mở rộng của Phương pháp nội suy điểm hướng kính (RPIM). Điểm thu hút của hàm dạng RPIM đó là nó sở hữu thuộc tính Kronecker delta, do đó có thể áp đặt trực tiếp các điều kiện biên cần thiết. Trong dạng mở rộng, bước nhảy trong trường độ võng và góc xoay do vết nứt gây ra, cũng như sự suy biến ứng suất gần đỉnh vết nứt được mô tả bằng cách thêm các hàm làm giàu vào phương trình nội suy. Cụ thể là hàm Heaviside và hàm làm giàu lân cận đỉnh vết nứt. Đối với tích phân số, Phương pháp biến đổi Đê-các (CTM) được sử dụng. Trong CTM không cần ô tích phân nền, kỹ thuật này biến tích phân miền thành tích phân trên biên và tích phân 1D. Để phân tích các bài toán không liên tục, trong nghiên cứu này, sự phân bố của các điểm tích phân được điều chỉnh để tránh sự gián đoạn gây ra bởi vết nứt. Do đó, không cần sử dụng miền con giống như các nghiên cứu CTM khác. Để đạt được điều này, một biên ảo được đưa vào để đại diện cho sự không liên tục của miền bài toán như lỗ hoặc vết nứt. Điều này cũng phù hợp với quan điểm của cách tiếp cận mở rộng rằng không tồn tại sự gián đoạn rõ ràng trong hình học của bài toán, thay vào đó, sự gián đoạn được mô hình hóa bằng phương trình toán học. Hệ số cường độ ứng suất (SIFs) của bài toán nứt được đánh giá thông qua kỹ thuật tích phân tương tác. Hiệu quả của phương pháp đề xuất được minh họa thông qua các ví dụ số khác nhau. Độ chính xác của các kết quả thu được được so sánh với các kết quả số và kết quả giải tích có sẵn khác.

Từ khoá: Phân tích nứt, phương pháp không lưới mở rộng, XRPIM, CTM

¹Bộ môn Cơ kỹ thuật, Khoa Khoa học ứng dụng, Trường Đại học Bách Khoa TP.HCM

²Đại học Quốc gia Thành phố Hồ Chí Minh

Liên hệ

Nguyễn Thanh Nhã, Bộ môn Cơ kỹ thuật, Khoa Khoa học ứng dụng, Trường Đại học Bách Khoa TP.HCM

Đại học Quốc gia Thành phố Hồ Chí Minh

Email: nhanguyen@hcmut.edu.vn

Lịch sử

- Ngày nhận: 16-12-2022
- Ngày chấp nhận: 09-9-2023
- Ngày đăng: 31-12-2023

DOI:



Bản quyền

© ĐHQG Tp.HCM. Đây là bài báo công bố mở được phát hành theo các điều khoản của the Creative Commons Attribution 4.0 International license.



Trích dẫn bài báo này: Vỹ L S, Hiền N T, Thiện T T, Nhã N T. Phân tích nứt bằng một phương pháp không lưới mở rộng và phương pháp biến đổi Đê-các không cần tạo miền con. *Sci. Tech. Dev. J. - Eng. Tech.* 2023, 5(S12):33-43.